Analysis of Cylindrical Transmission Lines with the Method of Lines

Shujun Xiao, Rüdiger Vahldieck, *Senior Member, IEEE,* and Jan Hesselbarth

Abstract— **Cylindrical transmission lines are important for a variety of applications. To calculate their propagation characteristics, the method of lines in cylindrical coordinates has been adopted. By discretizing the angular space direction with radial lines, the two-dimensional (2-D) Helmholtz equation reduces to a set of ordinary one-dimensional (1-D) differential equations, which can be solved analytically in radial direction after an orthogonal transformation. To improve the accuracy of the cylindrical method of lines from second-order to fourth-order, neighboring lines are used to eliminate second-order discretization errors not only in the Helmholtz equation but also in the continuity equation and in the edge condition. The method is suitable for the analysis of asymmetric cylindrical homogeneous and inhomogeneous guided wave structures.**

I. Introduction

CYLINDRICAL multiconductor transmission lines on soft substrate are of interest for a variety of applications, in particular for new types of antennas and their feed lines in mobile communication. The design of passive circuits on curved surfaces is not a simple problem and is difficult with most existing numerical approaches, especially when there is no angular symmetry. Several papers on this topic have been published so far. Most of them, however, are based on conformal mapping techniques (i.e., [1]–[4]) and are limited in their investigation to the fundamental quasi-TEM mode only. An exception are papers [5], [6] where higher order modes have also been analyzed.

In this paper we present a fullwave analysis of homogeneously filled cylindrical waveguides as well as planar transmission lines on a cylindrical dielectric body using the method of lines (MoL) in cylindrical coordinates. The advantages of the MoL (no relative convergence, semianalytical approach to solve the Helmholtz equation) have so far mostly been exploited for structures that fit into a rectangular coordinate system (i.e., [7], [8]). From that work the MoL is well known as a numerically efficient and versatile analysis method. Only little work has been done up to now to adopt this method also for cylindrical structures. In [9] the MoL based on Cartesian coordinates was utilized to analyze cylindrical structures. This led to a staircase approximation of the cylindrical metallic boundary, and in this case the method does not provide much of an advantage over other space discretization methods that use a rectangular or triangular mesh structure. To overcome this problem, Thorburn, Agostron, and Tripathi [10], [11] discretized the r-variables in the Helmholtz equation with circular lines and successfully solved the remaining equations along the θ-direction. However, they did not elaborate on how to solve the problem at $r = 0$ (center of the coordinate system) for the general case, that is, when no electric or magnetic walls can be assumed. This problem is avoided in [12], in which it is suggested to discretize the θ-variable instead of the r-variable by using radial straight lines. However, only angular symmetrical structures were tested, which is a special case. It was found that in this case the difference operator $[P]$, the eigenvalues $[\lambda]$, and the transformation matrix $[T]$ found for Cartesian coordinates (to diagonalize the Helmholtz equation) can also be applied to cylindrical coordinates. For asymmetric cylindrical structures this is not true since magnetic and electric walls can not be defined and the difference operator $[P]$ as well as the transformation matrix $[T]$ are different from [12], but identical to the ones developed for periodic structures in Cartesian coordinates [8].

If a waveguide structure is subdivided into homogeneous subregions, the continuity condition of fields between subregions must also be satisfied. For asymmetrical cylindrical structures this procedure has been described briefly in [16]. In the following we will address this problem in more detail in the context of numerical accuracy. It is well known that the MoL provides only second-order accuracy. To obtain fourth-order accuracy three neighboring lines must be utilized to eliminate analytically the second-order error. This was first shown in [7] for Cartesian coordinates, but in that work the fourth-order scheme was only applied to the discretization of the Helmholtz equation and no overall improvement of the MoL accuracy was achieved.

In [15] it was then demonstrated for the first time that in order to improve the overall accuracy of the Cartesian MoL the fourth-order scheme must also be applied to the continuity condition and the edge condition. In [16] the fourth-order scheme was then implemented also into the cylindrical MoL. Another higher order scheme was published recently [17], but only negligible improvement over the fourth-order scheme was demonstrated.

To further improve the computational efficiency of the cylindrical MoL the singular value decomposition (SVD) technique is utilized to find the zeros of the system determinant. The efficiency of the MoL algorithm in general is suffering from the fact that the system determinate contains poles and zeros and that they can be located in close proximity. Any root finding algorithm must distinguish between a zero and a pole. This is not only time consuming but can also lead to errors

Manuscript received July 25, 1994; revised March 20, 1996.

The authors are with the Laboratory for Lightwave Electronics, Microwave and Communications, Department of Electrical and Computer Engineering, University of Victoria, Victoria, B. C., V8W 3P6 Canada.

IEEE Log Number S 0018-9480(96)04698-4.

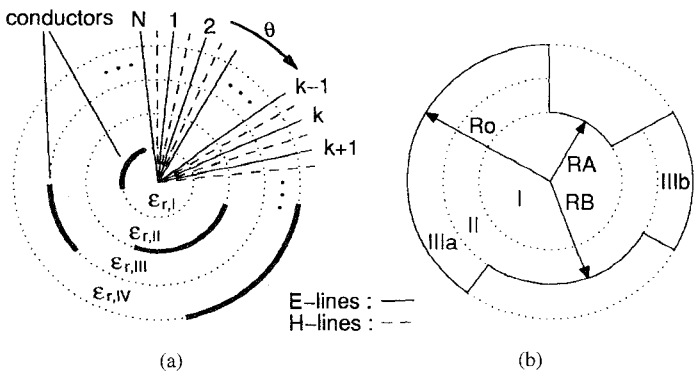

Fig. 1. (a) Discretization scheme for the CMoL in a multiconductor and multilayer cylindrical transmission line. (b) Circular ridge waveguide structure as an example for a cross-section with finite metallization thickness.

in that one or more zeros may not be found. Using an SVD algorithm eliminates this problem, as was shown in [13].

To test the cylindrical MoL (CMoL) algorithm, a variety of cylindrical cross sections have been calculated. Comparisons with numerical data from other methods shows generally good agreement and confirms the efficiency of this approach.

II. Semianalytical Solution of Helmholz Equation

The principal steps in developing the MoL algorithm are always th same, whether Cartesian or cylindrical coordinates are involved. Therefore, the following mathematical steps are greatly abbreviated and focus only on the aspects pertaining to the MoL in cylindrical coordinates. To outline the CMoL procedure the following discussion concentrates on planar transmission lines on curved multilayered dielectric substrate enclosed in a metallic cylindrical waveguide. The extension of the CMoL to radially open structures is straightforward.

The electromagnetic fields in each uniform region can be derived from two independent scalar potential functions $\phi_{e,h}\exp\{j\omega t-\gamma z\}$. Both are directly proportional to the field components E_z and H_z and satisfy the Helmholtz equation in polar coordinates

$$\frac{1}{r}\frac{\partial}{\partial r}\left(r\frac{\partial\phi}{\partial r}\right)+\frac{\partial^2\phi}{r^2\partial\theta^2}+(k^2-\beta^2)\phi=0 \tag{1}$$

as well as the boundary conditions depending on the structure ($k^2=\omega^2\mu\epsilon$).

The cross section of Fig. 1(a) is discretized in the θ-direction by using N radial lines

$$\theta_k=\theta_1+(k-1)h=\frac{2\pi k}{N},\qquad k=1,2,\cdots,N \tag{2}$$

with h being the angular spacing between the lines. The discretization lines for the electric potential function ϕ_e are shifted with respect to ϕ_h (the magnetic potential function) by half a discretization step, $h/2$. The first-order finite difference equation can then be written in matrix form as

$$h\frac{\partial\bar{\phi}_e}{\partial\theta}\cong[D]\bar{\phi}_e,\qquad h\frac{\partial\bar{\phi}_h}{\partial\theta}\cong-[D]^t\bar{\phi}_h \tag{3}$$

with $h=2\pi/N$. Vectors $\bar{\phi}_{e,h}$ denote $\bar{\phi}=[\phi_1\ \phi_2\ \phi_3,\cdots,\phi_N]^t$. The first-order finite difference operator $[D]$ is an $N\times N$ bidiagonal matrix identical to the one developed for periodic structures in [8], but different from the one used in [12] for symmetrical structures in that the lower left corner element of $[D]$ is 1 instead of zero. Using the central finite difference scheme again, the second-order partial differential operator yields

$$h^2\frac{\partial^2\bar{\phi}_e}{\partial\theta^2}\bigg|_i=(-[D]^t)[D]\bar{\phi}_e=[P]\bar{\phi}_e \tag{4}$$

and similarily for $\bar{\phi}_h$ with $[P]=[D](-[D]^t)=(-[D]^t)[D]$

$$[P]=\begin{bmatrix}2&-1&0&\cdots&0&0&-1\\-1&2&-1&\cdots&0&0&0\\\cdots&\cdots&\cdots&\cdots&\cdots&\cdots&\cdots\\\cdots&\cdots&\cdots&\cdots&\cdots&\cdots&\cdots\\0&0&0&\cdots&-1&2&-1\\-1&0&0&\cdots&0&-1&2\end{bmatrix}. \tag{5}$$

Due to the angular periodicity, $[P]$ contains a -1 element in the lower left and upper right corners, which again is not the case for symmetrical structures [12]. Introducing $[P]$ into the Helmholtz equation, a set of coupled ordinary differential equations is obtained

$$r\frac{d}{dr}\left(r\frac{d\bar{\phi}}{dr}\right)+k_c^2r^2\bar{\phi}-\frac{[P]\bar{\phi}}{h^2}=\bar{\gamma}$$

$$\bar{\gamma}=\frac{h^2}{12}\frac{\partial^4\bar{\phi}}{\partial\theta^4}+\frac{h^4}{360}\frac{\partial^6\bar{\phi}}{\partial\theta^6}+o(h^6) \tag{6}$$

where $k_c^2=k^2-\beta^2$ and γ is an error term. In order to decouple (6), $[P]$ must be diagonalized by an orthogonal matrix $[T]$ such that $[\lambda]=[T]^t[P][T]$ with $[T]^t=[T]^{-1}=[T]$, where $[\lambda]$ is a diagonal matrix of the eigenvalues of $[P]$. This can be achieved either with the complex transformation of [8], found for periodic structures, or with the following matrix:

$$T_{ij}=(\cos\alpha_{ij}+\sin\alpha_{ij})/\sqrt{N},\qquad \lambda_k=2(1-\cos\alpha_k) \tag{7}$$

where λ_k are the eigenvalues of $[P]$ and $\alpha_{ij}=h\cdot i\cdot j$, $h=2\pi/N$, $\alpha_k=h\cdot k$ $(i,j,k=1,2,\cdots,N)$. Applying this transform to (6) and substituting $\mu_k^2=\lambda_k/h^2$, the set of Helmholtz equations is now decoupled into a set of independent ordinary differential equations

$$\frac{d}{rdr}\left(r\frac{d\varphi_k}{dr}\right)+\left(k_c^2-\frac{\mu_k^2}{r^2}\right)\varphi_k=\bar{\gamma},\qquad \mu_k=\frac{2\sin(\alpha_k/2)}{h} \tag{8}$$

where φ_k $(k=1,2,3,\cdots,N)$ is called the *transformed potential function* and $\bar{\varphi}=[\varphi_1,\varphi_2,\cdots,\varphi_N]=[T]\bar{\phi}$. In every uniform region, the general solution to the Bessel equation (8) are Bessel functions of μ_k order

$$\varphi_k=A_kY_{\mu_k}^{(1)}(k_cr)+B_kY_{\mu_k}^{(2)}(k_cr) \tag{9}$$

where $Y_{\mu_k}^{(1,2)}$ is either one of the following functions:

$$Y_{\mu_k}^{(1)}(k_c r) \sim J_{\mu_k}(k_c r),\ I_{\mu_k}(k_c r),\ H_{\mu_k}^{(1)}(k_c r),$$

$$Y_{\mu_k}^{(2)}(k_c r) \sim N_{\mu_k}(k_c r),\ K_{\mu_k}(k_c r),\ H_{\mu_k}^{(2)}(k_c r).$$

J_{μ_k} and N_{μ_k} are, respectively, the Bessel functions of first and second kind. I_{μ_k} and K_{μ_k} are the modified Bessel functions of the first and second kind, and $H_{\mu_k}^{(1)}$ and $H_{\mu_k}^{(2)}$ are Hankel functions. These functions are selected according to the individual applications. For example, it should be noted that at $r = 0$ (the origin), N_{μ_k} and K_{μ_k} will be singular (approaching infinity). Therefore, for a problem including the region $r = 0$, these functions must be excluded. Similarly, for a region extended to infinity, the modified Bessel function of the first kind is excluded. For closed structures the telegraphist equation in polar coordinates is obtained as follows;

$$\begin{bmatrix} \varphi_k(k_c r_1) \\ \frac{1}{k_c}\frac{d\varphi_k(k_c r_1)}{dr} \end{bmatrix} = [w(J_{\mu_k}(k_c r_1),\ N_{\mu_k}(_c r_1))] \cdot [w(J_{\mu_k}(k_c r_2),\ N_{\mu_k}(k_c r_2))]^{-1} \times \begin{bmatrix} \varphi_k(k_c r_2) \\ \frac{1}{k_c}\frac{d\varphi_k(k_c r_2)}{dr} \end{bmatrix} \quad (10)$$

where

$$[w(y_1,\ y_2)] = \begin{bmatrix} y_1 & y_2 \\ y_1' & y_2' \end{bmatrix}.$$

The prime denotes a derivative with respect to r. Equation (10) links the transformed potential as well as its derivatives at the outer and inner boundaries of a homogeneous subregion. To link the fields between homogeneous subregions, the tangential field continuity condition must be applied.

III. Field Continuity Condition

For example, the continuity condition for E_θ after the discretization yields

$$\frac{\beta}{\omega\epsilon_0}[D]\left(\frac{\bar{\phi}_e^I}{\epsilon_{r,I}} - \frac{\bar{\phi}_e^{II}}{\epsilon_{r,II}}\right) = rh\left(\frac{d\bar{\phi}_h^{II}}{dr} - \frac{d\bar{\phi}_h^I}{dr}\right). \quad (11)$$

And similarly for the other field components. Multiplying $[T]^t$ and $[T]$ from the left and right sides, respectively, the above equation is diagonalized and yields one equation per line for the transformed potential φ. Relating these potentials to the conductor interface by using (10) and introducing the boundary conditions of tangential electric fields along the conductor surface, the relationship between the tangential fields E_z, E_θ and the surface current intensities J_z, J_θ at the interface can be obtained. Subsequently, all transformed potential functions and discretized tangential fields can be transformed back to the original domain to yield

$$[Z]\left[\bar{E}_z^I \bar{E}_\theta^I \bar{J}_z^{II} \bar{J}_\theta^{II}\right]^t = \left[\bar{J}_z^I \bar{J}_\theta^I \bar{E}_z^{II} \bar{E}_\theta^{II}\right]^t \quad (12)$$

where the superscripts I and II denote the fields at the interface between adjacent regions. Using the condition of zero tangential electric fields on metallic strips and zero current distribution in the slots, matrix equation (12) is reduced to

$$[Z]_{\text{red}}\left[\bar{E}_{z,\text{slot}}^I \bar{E}_{\theta,\text{slot}}^I \bar{J}_{z,\text{strip}}^{II} \bar{J}_{\theta,\text{strip}}^{II}\right]^t = 0. \quad (13)$$

For nontrivial solutions the zeros of $\det\{[Z]_{\text{red}}\} = 0$ must be found.

IV. Improved Accuracy of the Cylindrical MoL

In the previous paragraph we have outlined the basic MoL procedure in cylindrical coordinates. Obviously, the principle procedure is the same as in Cartesian coordinates except that all functions and variables are expressed in cylindrical coordinates. In the following we will show how the discretization error can be reduced to fourth-order by utilizing three neighboring lines in the discretization of the cylindrical Helmholtz equation as well as the discretized continuity condition. This was briefly described for the first time in [16].

As in any space discretization method the accuracy of the MoL depends mainly on the size of the discretization steps. Although a fine discretization improves the accuracy in general, also the CPU-time and memory space requirements increase. Alternatively, one can avoid small discretization steps to some degree if one can reduce the remaining finite difference error. The discretization error in the MoL is of second-order. To reduce this error to fourth-order is possible if three neighboring lines are included in the finite difference operator instead of only two. By choosing appropriate coefficients, the second-order error can be eliminated and only the fourth-order error remains. Since the MoL algorithm contains essentially three sources of discretization error (Helmholtz equation, continuity equation, and edge condition), the second-order error cancellation scheme must be applied to all three error sources in order to achieve an overall improvement in accuracy.

A. Helmholtz Equation

Discretizing the Helmholtz equation by using three neighboring lines yields

$$[Q]r\frac{d}{dr}\left(r\frac{d\bar{\phi}}{dr}\right) + k_c^2 r^2 [Q]\bar{\phi} - \frac{[P]\bar{\phi}}{h^2} = \bar{\gamma},$$

$$\bar{\gamma} = -\frac{h^4}{2\times 5!}\frac{\partial^6\bar{\phi}}{\partial\theta^6} + o(h^6) \quad (14)$$

where $[P]$ is the same as in (6), but a new matrix $[Q]$ occurs which is tridiagonal

$$[Q] = \frac{1}{12}\begin{bmatrix} 10 & 1 & 0 & \cdots & 0 & 0 & 1 \\ 1 & 10 & 1 & \cdots & 0 & 0 & 0 \\ \cdots & \cdots & \cdots & \cdots & \cdots & \cdots & \cdots \\ \cdots & \cdots & \cdots & \cdots & \cdots & \cdots & \cdots \\ 0 & 0 & 0 & \cdots & 1 & 10 & 1 \\ 1 & 0 & 0 & \cdots & 0 & 1 & 10 \end{bmatrix}. \quad (15)$$

The problem now is that (14) is a set of equations coupled not only through $[P]$ but also through $[Q]$. In order to solve (14) analytically, we must diagonalize $[P]$ and $[Q]$ with the same orthogonal matrix. Since $[Q] = [I] - \frac{1}{12}[P]$ and $[P]$ can be

diagonalized by $[T]$, it is found that matrix $[Q]$ can also be diagonalized by $[T]$ such that

$$[T]^t[Q][T] = \text{diag}\left[1 - \frac{\lambda_k}{12}\right] \tag{16}$$

where λ_k is given already in (7).

B. Field Continuity Equation

A Taylor series analysis at a specific line k reveals for the first derivative of the potential ϕ

$$\frac{\partial\phi_k}{\partial\theta} = \frac{1}{h}(\phi_{k+1} - \phi_k) - \frac{h^2}{24}\frac{\partial^3\phi_k}{\partial\theta^3} - \frac{h^4}{1920}\frac{\partial^5\phi_k}{\partial\theta^5} - \cdots. \tag{17}$$

The third-order derivative is approximated by the central difference quotient

$$\frac{\partial^3\phi_k}{\partial\theta^3} \approx \frac{\partial}{\partial\theta}\left(\frac{\phi_{k-1} - 2\phi_k + \phi_{k+1}}{h^2}\right) \tag{18}$$

which results in the following field continuity equation for E_θ, where the error of (h^2)-order is cancelled and the remaining error is therefore of fourth-order (h^4)

$$\bar{\gamma} = -\frac{17h^4}{2\times 4!\times 5!}\frac{\partial^5\bar{\phi}^{I,II}}{\partial\theta^5} + o(h^6). \tag{19}$$

Now the continuity equation, for example for E_θ, yields

$$\frac{\beta}{\omega\epsilon_0}[D]\left(\frac{\bar{\phi}_e^I}{\epsilon_{r,I}} - \frac{\bar{\phi}_e^{II}}{\epsilon_{r,II}}\right) = [U]hr\left(\frac{d\bar{\phi}_h^{II}}{dr} - \frac{d\bar{\phi}_h^I}{dr}\right) \tag{20}$$

where

$$[U] = \frac{1}{24}\begin{bmatrix} 22 & 1 & 0 & \cdots & 0 & 0 & 1 \\ 1 & 22 & 1 & \cdots & 0 & 0 & 0 \\ \cdots & \cdots & \cdots & \cdots & \cdots & \cdots & \cdots \\ \cdots & \cdots & \cdots & \cdots & \cdots & \cdots & \cdots \\ 0 & 0 & 0 & \cdots & 1 & 22 & 1 \\ 1 & 0 & 0 & \cdots & 0 & 1 & 22 \end{bmatrix}. \tag{21}$$

Because of $[U] = [I] - \frac{1}{24}[P]$, the matrix $[U]$ as well as $[D]$ can be diagonalized by $[T]$. Similar equations are obtained from the other field continuity conditions.

The application of the above procedure to the edge condition is straightforward. The above procedure is suitable only for cylindrical structures with metal strips of negligible thickness. To account for the finite metallization thickness, additional subregions must be introduced with transformation matrices $[T]$ that are determined by the boundary conditions in those regions. For Cartesian coordinates this procedure has been described in [8]. The implementation of this procedure in cylindrical coordinates has not been described before and will be outlined briefly in the following for the analysis of the structure shown in Fig. 1(b). This is a circular ridge waveguide (CRW) with different ridge depths. The CRW is divided into four subregions in which the discretized Helmholtz equation must be diagonalized individually. The difference to the diagonalization procedure described above is that the transformation matrices in regions IIIa and IIIb of Fig. 1(b) depend now on the boundary conditions of the side walls of both ridges, while $[T]$ in region II is only determined by the sidewalls of the ridge with larger penetration depth. In region I, $[T]$ is again determined by the periodic boundary condition. Because of the different transformation matrices, the matching of the fields at the interfaces between the subregions must be performed in the space domain [8]. This was not necessary for the cylindrical microstrip structures with thin metal strip ($[T]$ was the same in all subregions). Transforming the fields of the center section I into the interface determined by radius RA leads to

$$\begin{bmatrix} j\omega\mu_0 k_c H_z(RA) \\ \omega\mu_0 H_\theta(RA) \end{bmatrix} = \begin{bmatrix} k_c^2 X_h & \frac{\beta}{hRA}X_h D_e \\ -\frac{\beta}{hRA}D_h X_h & -\epsilon_r k_0^2 X_e - \left(\frac{\beta}{hk_cRA}\right)^2 D_h X_h D_e \end{bmatrix} \cdot \begin{bmatrix} E_\theta(RA) \\ jE_z(RA) \end{bmatrix} \tag{22}$$

$$X_\epsilon = T\cdot\text{diag}\left[\frac{J'_\mu(k_cRA)}{J_\mu(k_cRA)}\right]\cdot T^t$$

$$X_h = T\cdot\text{diag}\left[\frac{J_\mu(k_cRA)}{J'_\mu(k_cRA)}\right]\cdot T^t. \tag{23}$$

The transformation matrices of the other subsections are similar, although more complex because of the different boundary conditions for the E- and H-fields and the fact that cylindrical functions of both the first and the second kind have to be taken into account. In cases where $k_c^2 < 0$, the Bessel functions J and N are replaced by the modified Bessel functions I and K, respectively.

For a waveguide homogeneously filled with a dielectric, only the cutoff frequencies of the modes need be calculated. Then, for $\beta = 0$, the above matrix equation separates into two uncoupled matrix equations of only one quarter of the original size—one for TE modes and one for TM modes.

V. SVD and Eigenvalue Solution Procedure

The fourth-order scheme discussed above does not change the principal composition of the system matrix $[Z]$ in (13) or (23). To find the nontrivial solutions of $[Z]$ can be time consuming since poles and zeros may be in close proximity and are therefore difficult to distinguish. As shown in [13] for the mode matching method, the singular value decomposition (SVD) procedure may be used to eliminate this problem. To do so, the system matrix $[Z]$ is diagonalized by two unitary matrices, $[F]$ and $[V]$ ($[F]^h[F] = [I]$ and $[V]^h[V] = [I]$, where $[I]$ is an identity matrix and the superscript h denotes Hermitian conjugate) such that $[F]^h[Z][V] = [S]$. $[S]$ is the resulting diagonal matrix whose elements are called singular values of matrix $[Z]$. For simplicity we rewrite (13) as $[Z]a = b$, or in its diagonalized form as $[S]A = B$, where $A = [V]^h a$ and $B = [F]^h b$. The lowest singular value approaching zero will now be exactly equivalent to (13). The modal field and current distribution can then be obtained from $[F]$ and $[V]$ at the minima of the lowest $S_{\min} - > 0$. In other words, the eigenvalue search in the MoL algorithm is now equivalent to finding all the local minimum points of the lowest singular

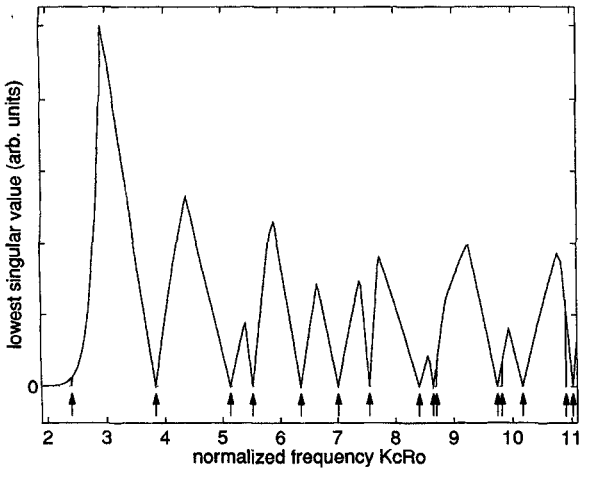

Fig. 2. Evaluation of the lowest singular values of the eigenvalue matrix for TM modes of a cylindrical waveguide. Sixty lines used in the discretization of the waveguide cross-section.

values of $[Z]$ along the frequency axis by using a one-dimensional (1-D) line search method. Poles are thus avoided and present no problem for the search algorithm. This is shown graphically in Fig. 2 for the cutoff frequencies of the TM modes in a hollow circular waveguide. This simple structure was chosen to compare the numerical results with analytical solutions.

VI. Numerical Results

In order to test the cylindrical MoL algorithm with fourth-order accuracy, a variety of structures have been investigated and compared with other methods. First of all, Fig. 3(a) illustrates the advantages of using the scheme with fourth-order accuracy over the one with only second-order accuracy. To reach the same accuracy of the fourth-order scheme, it is apparent that the second-order scheme requires approximately twice the number of lines.

In comparison with other methods, the cylindrical MoL is generally in good agreement, as shown in Fig. 3(b) and (c) for the propagation constant and the characteristic impedance, respectively. Some discrepancies with quasistatic results, however, can be observed in Fig. 4. It appears as if the dispersion is more pronounced in the microstrip line on curved than on plane substrate, which would explain the deviations from [3] in which a conformal mapping technique was used. For a bilateral finline structure shielded by a circular waveguide housing (Fig. 5), results are compared with the finite element analysis [14] and the Cartesian MoL [9]. As demonstrated in Fig. 5, also here the agreement is very good for the fundamental and higher order modes.

For circular ridge waveguides, results are shown in Figs. 6 and 7. Fig. 6 illustrates the convergence behavior of the cutoff frequencies for the first 25 TM modes. It is evident that with increasing mode number the number of lines must increase to maintain a certain error level. To give an example for the specific ridge constellation shown in Fig. 6, the TM21 modes are determined with only 30 lines to less than 0.2% accuracy, while for the TM03 mode 90 lines are required.

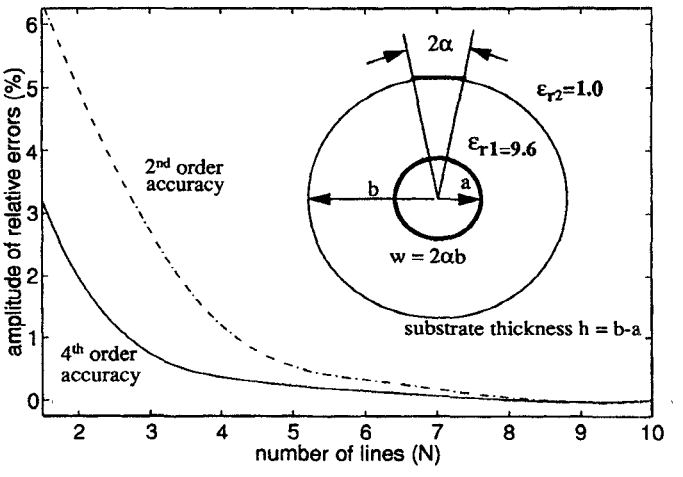

(a)

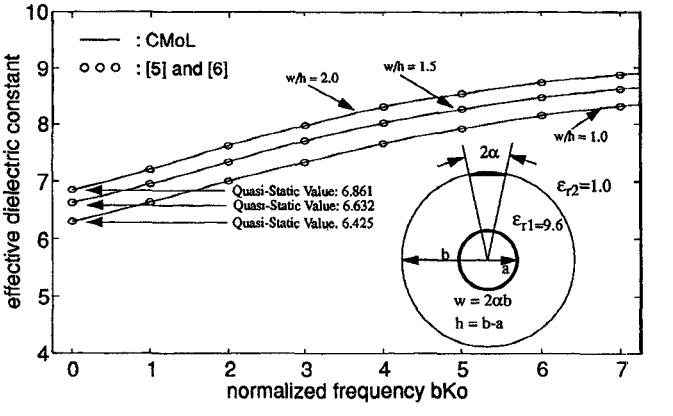

(b)

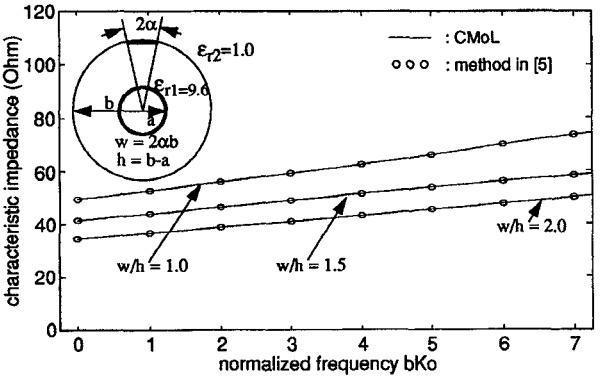

(c)

Fig. 3. Frequency-dependent properties of an open cylindrical microstrip line. $\epsilon_{r1} = 9.6$, curve-linear coefficient $R = a/b = 0.9$. (a) Convergence test, (b) ϵ_{eff} versus frequency, and (c) characteristic impedance versus frequency.

Higher modes need a correspondingly higher number of lines. Similar convergence behavior is observed for TE modes.

Fig. 7 shows the change in cutoff frequency for the first TE modes when the penetration depths of both ridges increases. Two effects can be observed: First, because of the asymmetric structure, all of the orthogonally polarized TE modes separate, and second, when mode crossing occurs the numerical results

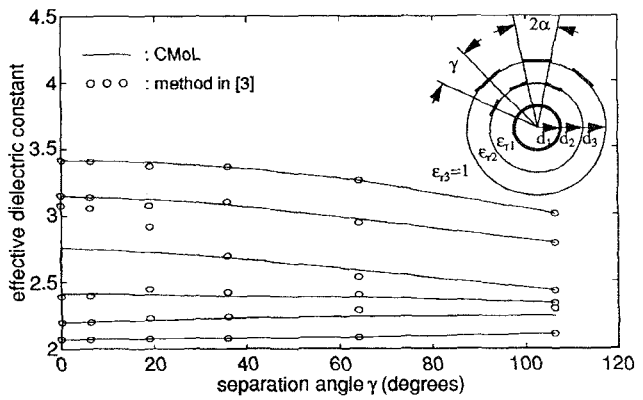

Fig. 4. Effective dielectric constant of an open multiconductor microstrip line versus the separation angle γ. Dimensions of the different layers: $d_3/d_1 = 3$, $d_2/d_1 = 2$, $\epsilon_{r1} = 2$, $\epsilon_{r2} = 4$, $\epsilon_{r3} = 1$, $\alpha = 10.195^0$.

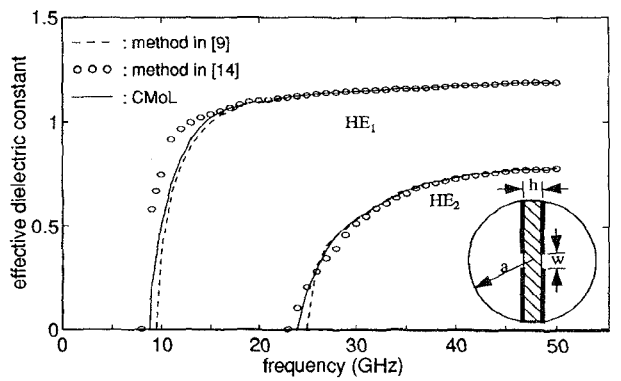

Fig. 5. Dispersion characteristic of a bilateral finline in a circular waveguide enclosure. Waveguide housing WC-33, $a = 4.165$ mm, $h = 0.254$ mm, $w = 0.3$ mm, $\epsilon_r = 2.2$.

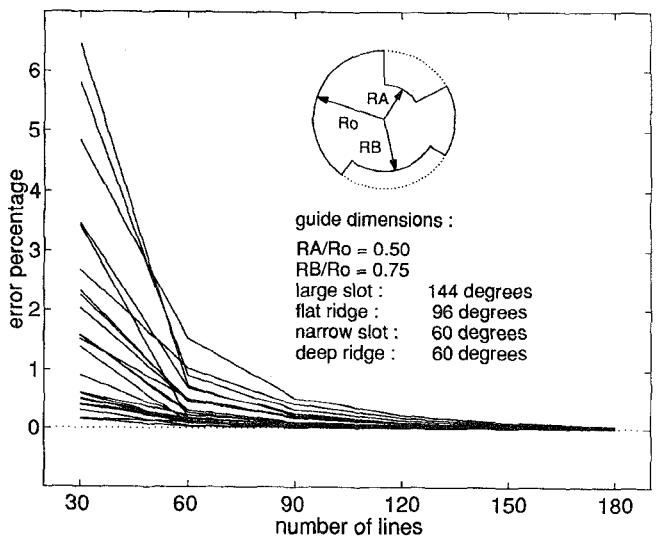

Fig. 6. Convergence test for TM modes in a CRW.

from the SVD procedure indicate otherwise, as shown in the inset. A fine resolution of the SVD results in the neighborhood of the cross-over point suggests that there is no mode crossing. However, plotting the fields of the modes a distance away from the cross-point indicates clearly that the modes must have crossed.

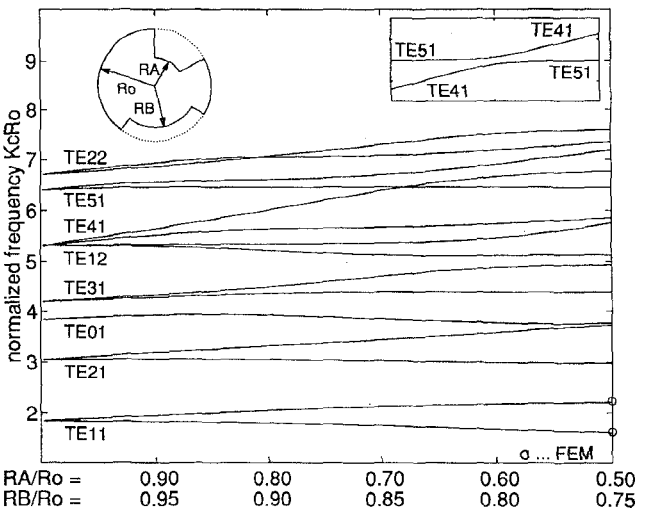

Fig. 7. Cutoff frequencies of TE modes versus ridge penetration depths.

VII. Conclusion

The method of lines in cylindrical coordinates (CMoL) has been described for angular asymmetric structures including finite metallization thickness. The accuracy of the CMoL has been improved from second-order to fourth-order in all three sources of error, that is, the Helmholtz equation, the continuity condition, and the edge condition. The method has been tested for inhomogeneous (multilayered dielectric structures) asymmetric transmission lines and homogeneous circular ridge waveguides.

References

[1] L. R. Zeng and Y. X. Wang, "Accurate solutions of elliptical and cylindrical striplines and microstrip lines," *IEEE Trans. Microwave Theory Tech.*, vol. MTT-34, no. 2, pp. 259–265, Feb. 1986.

[2] C. J. Reddy and M. D. Deshpande, "Analysis of cylindrical stripline with multilayer dielectrics," *IEEE Trans. Microwave Theory Tech.*, vol. MTT-34, no. 6, pp. 701–706, June 1986.

[3] C. H. Chan and R. Mittra, "Analysis of a class of cylindrical multiconductor transmission lines using an iterative approach," *IEEE Trans. Microwave Theory Tech.*, vol. MTT-35, no. 4, pp. 415–424, Apr. 1987.

[4] S. S. Bedir and I. Wolff, "Extending the use of conformal mapping technique for the calculation of the quasi-TEM parameters of several cylindrical and wrapped transmission lines," in *1989 IEEE MTT-S Int. Microwave Symp. Dig.*, Long Beach, CA, 1989, pp. 1127–1130.

[5] N. Alexopoulos and A. Nakatani, "Cylindrical substrate microstrip line characterization," *IEEE Trans. Microwave Theory Tech.*, vol. MTT-35, no. 9, pp. 843–849, Sept. 1987.

[6] A. Nakatani and N. Alexopoulos, "Coupled microstrip line on cylindrical substrate," *IEEE Trans. Microwave Theory Tech.*, vol. MTT-35, no. 12, pp. 1392–1398, Sept. 1987.

[7] U. Schulz, "A new technique for the analysis of planar microwave structures," Ph.D. dissertation, Fern Univ., Hagen, Germany, 1980.

[8] R. Pregla and W. Pascher "The method of lines," T. Itoh, Ed., in *Numerical Techniques for Microwave and Millimeter-Wave Passive Structures*. New York: Wiley, 1989, pp. 381–446.

[9] K. Wu and R. Vahldieck, "The method of lines applied to planar transmission lines in circular and elliptical waveguides," *IEEE Trans. Microwave Theory Tech.*, vol. 37, no. 12, pp. 1958–1963, Dec. 1989.

[10] M. Thorburn, A. Agostron, and V. K. Tripathi, "Computation of frequency-dependent propagation characteristics of microstriplike propagation structures with discontinuous layers," *IEEE Trans. Microwave Theory Tech.*, vol. 38, no. 2, pp. 148–153, Feb. 1990.

[11] M. Thorburn, A. Biswas, and V. K. Tripathi, "Application of method of lines to cylindrical inhomogeneous propagation structures," *Electron. Lett.*, vol. 26, no. 3, pp. 170–171, 1990.
[12] Y. Xu, "Application of the method of lines to solve problems in cylindrical coordinates," *Microwave Opt. Technol. Lett.*, vol. 1, no. 5, pp. 173–175, July 1988.
[13] V. A. Labay and J. Bornemann, "Matrix singular decomposition for pole-free solutions of homogeneous matrix equation as applied to numerical modeling methods," *IEEE Microwave and Guided Wave Lett.*, vol. 2, no. 2, pp. 55–57, 1992.
[14] Eswarappa, G. I. Costache, and W. J. R. Hoefer, "Finlines in rectangular and circular waveguide housings including substrate mounting and bending effects-finite element analysis," *IEEE Trans. Microwave Theory Tech.*, vol. 37, no. 2, pp. 299–306, Feb. 1989.
[15] S. Xiao, R. Vahldieck, H. Jin, and Z. Cai, "A modified MoL algorithm with faster convergence and improved computational efficiency," in *1991 IEEE MTT-S Int. Microwave Symp. Dig.*, Boston, June 1991, pp. 357–360.
[16] S. Xiao and R. Vahldieck, "Full-wave characterization of cylindrical layered multiconductor transmission lines using the MoL," in *1994 IEEE MTT-S Int. Microwave Symp. Dig.*, San Diego, CA, May 1994, pp. 149–152.
[17] R. Pregla, "Higher order approximation for the difference operators in the method of lines," *IEEE Microwave and Guided Wave Lett.*, vol. 5, no. 2, pp. 53–55, Feb. 1995.

Shujun Xiao was born April 1963 in P.R. China. He received the B.S.and M.S. degrees from the Department of Electrical Engineering, Beijing Institute of Tchnology (BIT), Beijing, P.R. China, in 1983 and 1986, respectively, and the Ph.D. degree from the Department of Electrical and Computer Engineering, University of Victoria (UVic), Victoria, B.C., Canada.

Currently, he is a Project Engineer with Allen Telecom, Reno, NV. His current interests are in RF design and communication systems, espcially filter and duplexer design for cellular and PCS base stations.

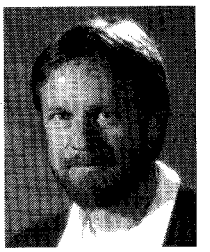

Rüdiger Vahldieck (M'85–SM'86) received the Dipl.-Ing. and the Dr.-Ing. degrees in electrical engineering from the University of Bremen, West Germany, in 1980 and 1983, respectively.

From 1984 to 1986 he was a Research Associate at the University of Ottawa, Canada. In 1986 he joined the University of Victoria, British Columbia, Canada, where he is now a Full Professor in the Department of Electrical and Computer Engineering. From 1992 to 1993 he was a Visiting Scientist at the Ferdinand-Braun-Institute für Hochfrequenztechnik, Berlin, Germany. His research interests include numerical methods to model electromagnetic fields for computer-aided design of microwave, millimeter wave, and optoelectronic integrated circuits. He is interested in design aspects of passive and active planar and quasiplanar components for MIC and MMIC applications and recently also in the design and simulation of broadband fiber-optic communication systems and subsystems.

Dr. Vahldieck, together with three coauthors, received the outstanding publication award of the Institution of Electronic and Radio Engineers in 1983. He is on the editorial board of the IEEE TRANSACTIONS ON MICROWAVE THEORY AND TECHNIQUES and has published more than 100 technical papers, mainly in the field of microwave CAD.

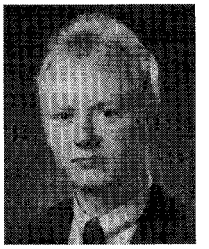

Jan Hesselbarth was born in Dresden, Germany, in 1970. He received the Dipl.-Ing. degree in 1995 from Dresden University of Technology.

From 1994 to 1995, he worked at the Ecole Nationale Superieure des Telecommunications, Paris, on sixport reflectometers. Since September 1995, he has been a Research Assistant at University of Victoria, British Columbia, working on numerical methods of solving wave propagation problems.